TIDC Transportation Infrastructure Durability Center AT THE UNIVERSITY OF MAINE

Comparison between Contact and Remote Crack Detection using GPR and SAR

Authors: Sanjana Vinayaka, Ahmed Alzeyadi

Department of Civil and Environmental Engineering, University of Massachusetts Lowell

Advisor: Dr. Tzuyang Yu

Introduction

Concrete cracking is a commonly seen durability issue of concrete bridges. While crack length and crack width can be statistically measured on the surface of concrete bridges, crack depth usually remains unknown to civil engineers without the use of destructive testing. On this poster, quantitative comparison between *contact* ground penetrating radar (GPR) and *remote* synthetic aperture radar (SAR) images on concrete crack detection is presented.

Experimentation

1. Specimen preparation

Four concrete panels (CNI, CNC, CNCD, CNCW) of dimensions 30x30x4 cm^3 were cast and artificial cracks were introduced at the center of three concrete panels. The dimensions of three artificial cracks are as shown in **Fig. 1**

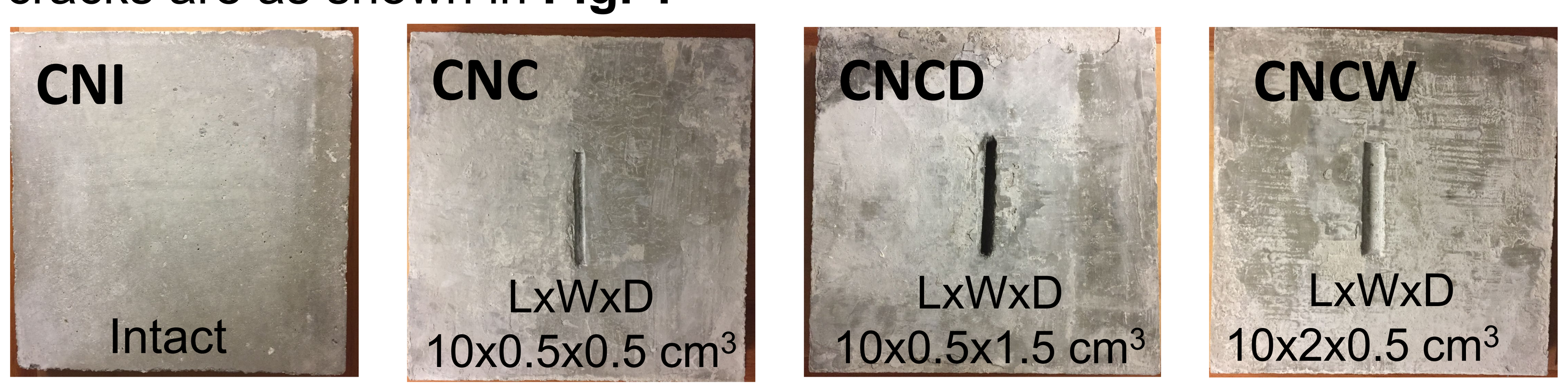

Fig. 1 Concrete panels with an artificial crack

2. Data collection

Four concrete panels were scanned using 10.5 GHz SAR imaging sensor inside an anechoic chamber. Laboratory SAR imaging facility and SAR images of four concrete panels are shown in **Fig. 2**. Reduction of SAR amplitudes was observed in **Fig. 2**. Also, a 1.6GHz GPR sensor was used to collect B-scan images in range—cross-range domain of four concrete panels, as shown in **Fig. 3**. Reduction in GPR amplitude was observed at the location of crack at 12, 24, 36 inches from the reference point.

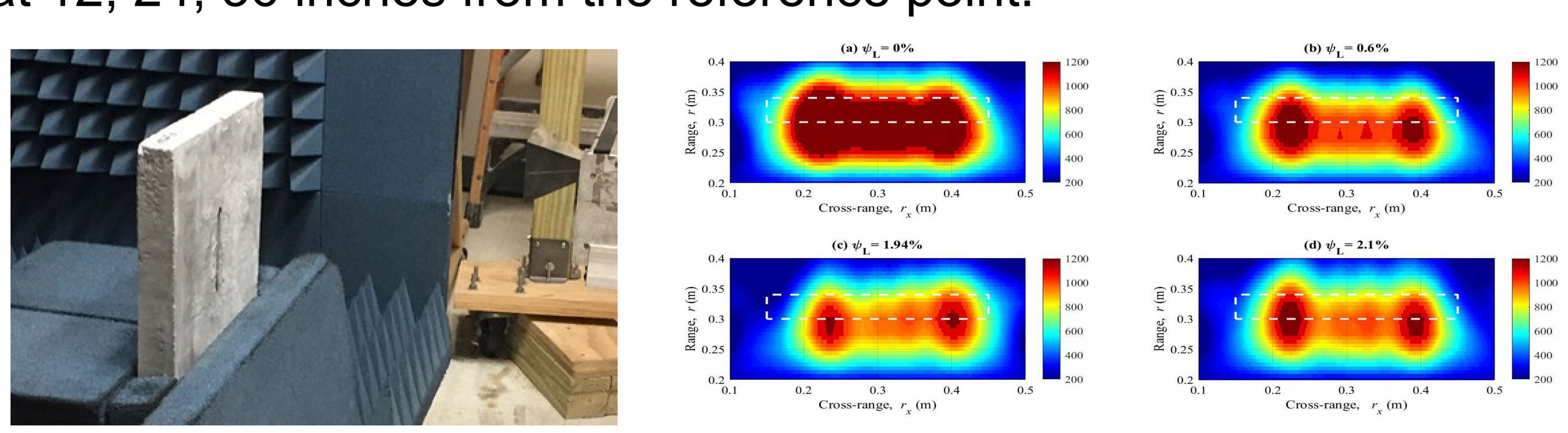

Fig. 2 Laboratory SAR imaging facility and SAR images of concrete specimens

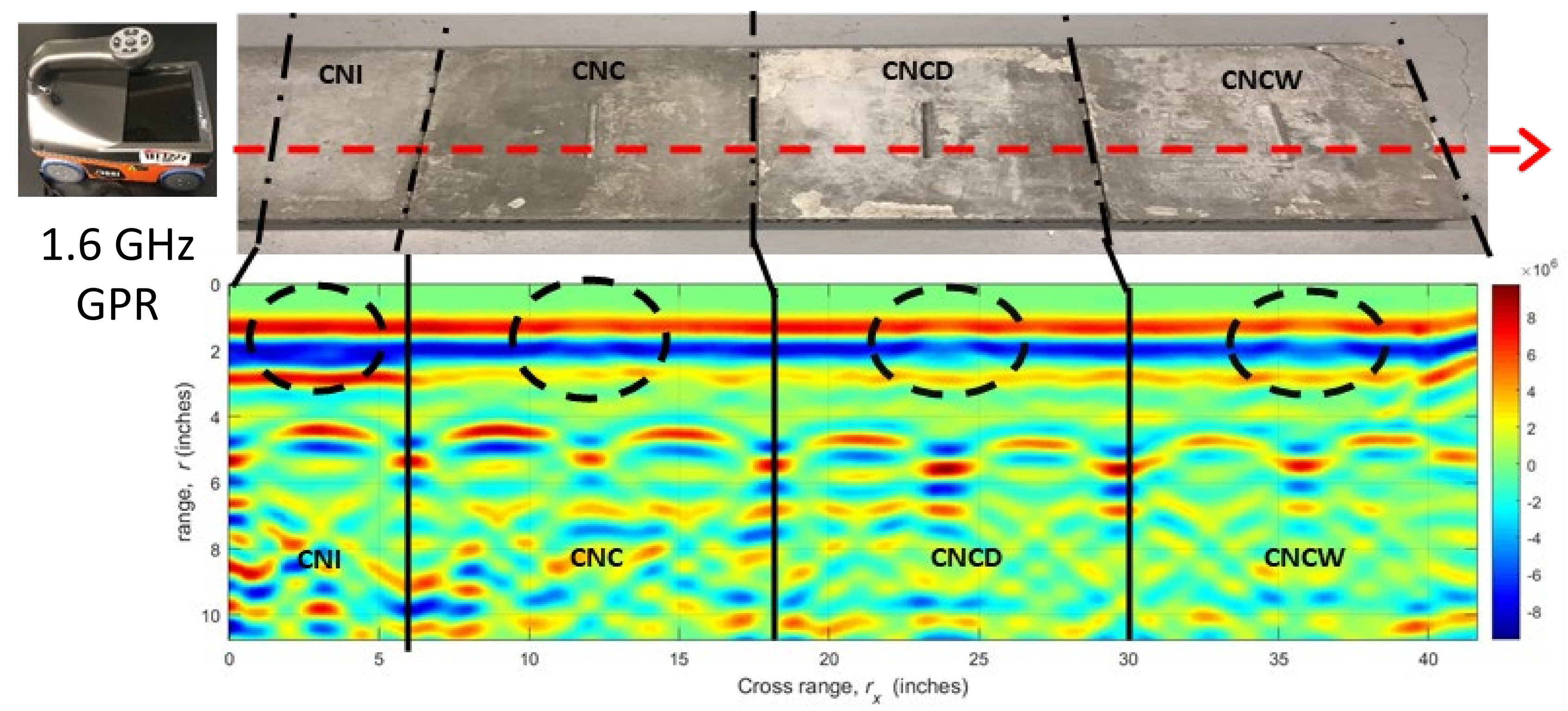

Fig. 3 GPR B-scan and its images of concrete panels

Crack detection

When GPR detects a surface crack in concrete, a hyperbolic pattern of reduced GPR amplitudes can be found (**Fig. 4**). When SAR detects the same surface crack in concrete from a distance, the background surface reflection (specular returns) is usually too strong to be used for damage detection. Rather, the backscattering signals are be amplified by the superposition of sub-images in SAR. This is manifested in change in SAR contours at three different SAR amplitudes as shown in **Fig.5. Fig. 6** compares the *contact* GPR inspection scheme with *remote* SAR inspection scheme. **Fig. 7** shows the hyperbolic scattering pattern in GPR images and the backscattering pattern in SAR images.

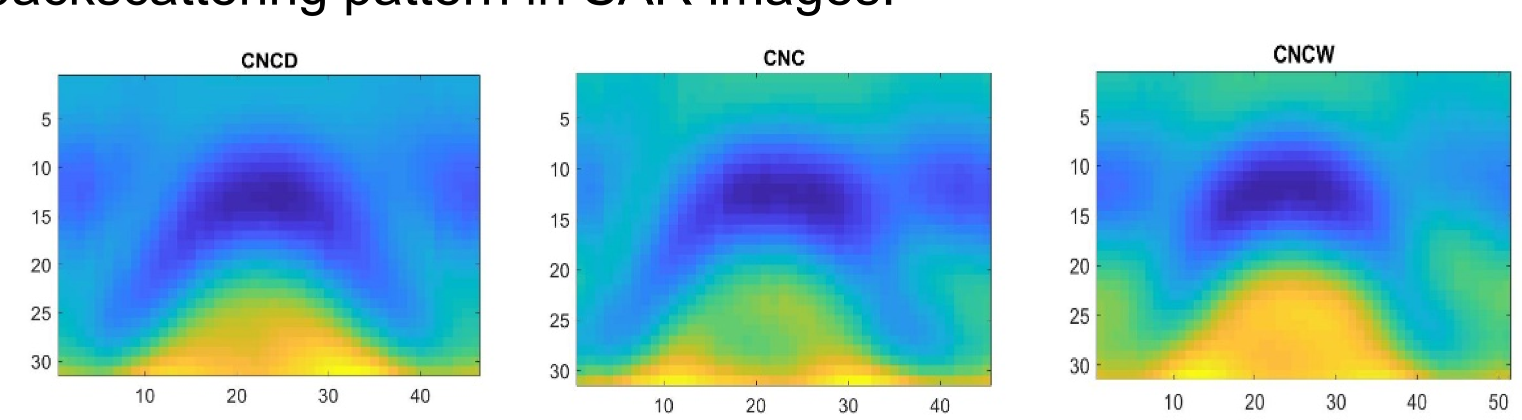

Fig. 4 GPR hyperbolic signal from the crack

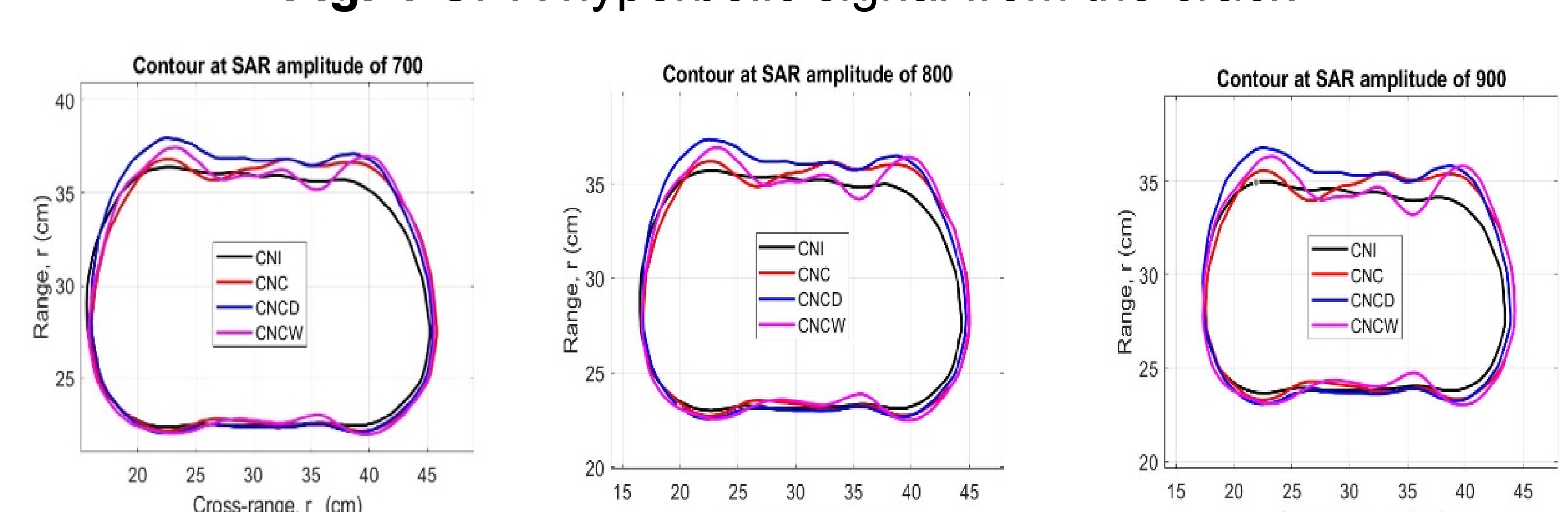

Fig. 5. SAR contours at three different SAR amplitudes (700, 800, and 900)

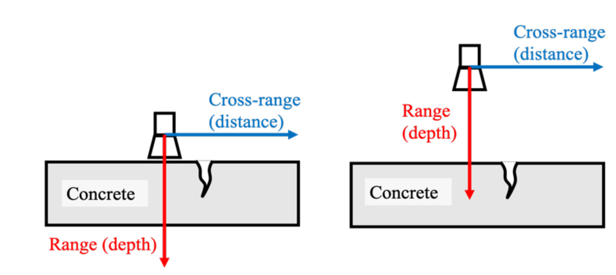

Fig. 6. GPR and SAR inspection schemes

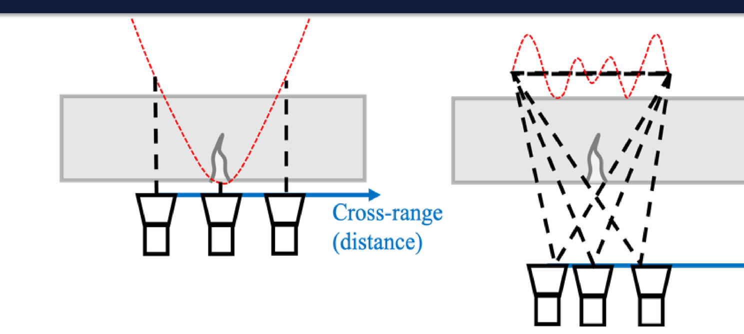

Fig. 7. GPR and SAR scattering pattern of cracks

Crack quantification

To better describe the continuous hyperbolic pattern in **Fig.4**, local minima points were extracted and modeled with a second order polynomial function. **Table. 1** summarizes modelling results. **Fig. 8** shows extracted hyperbolae with its characteristic width (w). Characteristic width (*w*) of the hyperbolae follows the pattern $w_{CNCW}>w_{CNCD}>w_{CNC}$ which is related to individual crack volumes. Finally, crack depth can be calculated from Eq. (1)

Table 1. Polynomial modelling of surface cracks

Specimen	CNC	CNCD	CNCW
2nd order polynomial equation	$y = 0.0431x^2 - 1.87x + 32.59$ ($R^2 = 0.9136$)	$y = 0.03918x^2 - 1.81x + 34.46$ ($R^2 = 0.9515$)	$y = 0.03606x^2 - 1.69x + 31.36$ ($R^2 = 0.9539$)
Curvature (k) = y'' (cm^{-1})	0.0862	0.0783	0.0721
1/k (cm)	11.6	12.7	13.8
Crack volume (V) (cm^3)	2.5	7.5	10

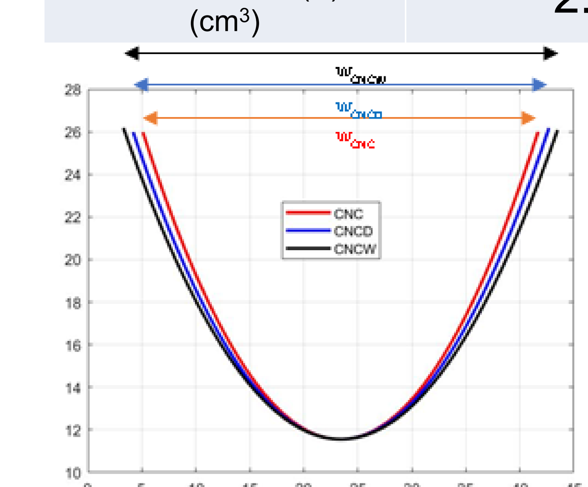

Fig. 8. Extracted hyperbolae with characteristic width (w)

$$D = \frac{\frac{1}{k} - 10.8}{0.2914 * L * W} \quad (1)$$

where D = crack depth (cm), *L* = crack length (cm), W = crack width (cm).

Conclusion

- Contact GPR and remote SAR can be used to i) detect the presence of a surface crack and ii) quantify crack depth on concrete panels.
- Presence of surface cracks will generate hyperbolic scattering in GPR images. For SAR images, a semi-sinusoidal pattern is observed.

University of Massachusetts Lowell UMASS

Contact: Prof. Tzuyang Yu at UML (tzuyang_yu@UML.EDU)

September 2020 – www.tidc-utc.org